International Journal of Thermal Sciences 221 (2026) 110492

Contents lists available at ScienceDirect

International Journal of Thermal Sciences

journal homepage: www.elsevier.com/locate/ijts

Loosely-coupled Conjugate Heat Transfer analysis of transient wall condensation

I. Rafanelli [a,*], A. Andreini [a], L. He [b]

[a] Department of Industrial Engineering, University of Florence, Florence, Italy
[b] Department of Engineering Science, University of Oxford, Oxford, United Kingdom

ARTICLE INFO

Keywords:
Conjugate heat transfer
Transient
Steam turbines
Dual time-step
Loosely coupled

ABSTRACT

The increasing integration of renewable energy sources into power generation systems has led steam turbines to operate more frequently under off-design conditions, with repeated start-ups and shutdowns introducing thermal transients that can compromise structural integrity. During cold start-up, the interaction between superheated steam and cold walls can trigger film condensation, releasing a large amount of energy and creating a strongly coupled problem between the film dynamics and the thermal response of the solid.

While various strategies have been proposed to address the mismatch in characteristic timescales between fluid and solid in Conjugate Heat Transfer (CHT) problems, the limitations of commonly used quasi-steady approaches has been rarely discussed.

In light of this, the novelty of this work lies in the development and validation, with both analytical solution and experimental data, of an equilibrium-based phase change model for laminar condensate films and in the demonstration of the inadequacy of widely adopted computational cost-saving strategies in turbomachinery applications, when dealing with thermal transients involving the transport of a laminar condensing film. Finally, the source terms based loosely-coupled Dual Time-Step method is adopted, showing a remarkable ability to predict the non negligible inertia that a condensing laminar film typically exhibits.

1. Introduction

The heat release due to phase change is a widely used phenomenon in numerous applications such as cooling of electronic components, electric vehicles, heat exchangers, and environmental cooling [1]. In particular, the advantage lies in the ability to remove a large amount of heat without the need for low cooling temperatures, thereby exploiting the high heat transfer coefficient that such a phenomenon typically involves. During the cold start of steam turbines, the opposite phenomenon occurs: when superheated steam comes into contact with a cold wall, the process of wall condensation is triggered. Tanasawa [2] highlighted that, depending on thermofluid dynamic conditions and wall treatment, two types of wall condensation can occur: *filmwise condensation*, which consists of a continuous and very thin film with a $O(100\ \mu m)$ thickness, which acts as a thermal resistance between the steam and the wall, and *dropwise condensation*, a topologically more complex phenomenon that involves a series of randomly distributed, growing, and coalescing drops. Referring to [2], it can be demonstrated that, given the high $(T_{sat} - T_w)$ values that typically occur during the startup of steam turbines, the predominant phenomenon in this phase is filmwise condensation. Moreover, Tancon et al. [3] conducted condensation experiments of water on an hydrophilic flat plate with films/droplets subjected to gravity and shear stress, finding that the transition from filmwise to dropwise condensation occurs at wall subcooling temperatures of approximately 5 K. This result is in line with Tanasawa [2], establishing filmwise condensation as the predominant phenomenon during most of the cold start-up phase of steam turbines. In this case, unlike evaporative cooling, a large amount of heat is transferred to the wall itself, leading to unavoidable thermal gradients on the solid domain. The impact of cold and hot start-up of steam turbines has been widely studied in the literature [4,5], highlighting that controlling the temperature evolution is necessary to ensure proper operation and prevent crack formation.

From a physical point of view, the boundary conditions of the condensate film balance equations strongly depend on the wall temperature. In fact, under the assumption of phase equilibrium, the condensate mass flow rate can be estimated using the Stefan boundary condition [6] in the continuity equation, thus inseparably linking the condensate flow rate to the temperature gradient across the film itself. On the other hand, the condensate flow rate is the main factor determining the amount of energy released to the solid. This highlights a

* Corresponding author.
E-mail address: isacco.rafanelli@unifi.it (I. Rafanelli).

https://doi.org/10.1016/j.ijthermalsci.2025.110492
Received 6 August 2025; Received in revised form 10 November 2025; Accepted 14 November 2025
Available online 25 November 2025

significant coupling between the thermal transient of the solid and the liquid film flow field.

Nowadays, computational fluid dynamics (CFD) plays a fundamental role in the design phase of turbomachinery components. Although numerous numerical and experimental studies have been proposed over the years to analyze the operation of steam turbines under both design and off-design conditions, from both a performance and structural integrity perspective, the authors highlight a lack of CFD investigation into the transient phenomenon of wall condensation, which is typical during the cold start-up phase of the machine. From an application standpoint, studying this phenomenon would not only allow for an estimation of the previously mentioned temperature gradients within the machine and the resulting stresses but would also provide important insights into the condensate mass flow rate generated throughout the entire transient. This information is crucial from a plant engineering perspective, as it allows a proper sizing of drainage pipes connected to the condenser. While under-sizing these pipes would lead to water accumulation within them, causing corrosion issues [7] and thermal load imbalances, over-sizing the drainage pipes would force the system to operate with cooling of the superheated steam in order to prevent hot vapor suction to the condenser.

Over the years, many approaches have been proposed for the study of multiphase flows with phase change. The first works proposed for estimating the condensate mass flow rate under ideal conditions are the steady-state analytical solution by Nusselt [8] and the multi-purpose time evolution of the interface described by the solution of the Stefan problem [9]. While the former describes the steady-state solution of a laminar film under ideal conditions (absence of shear stresses, vertical flat plate, vapor at saturation temperature, constant temperature on the plate), the latter describes the evolution of a quiescent liquid layer driven by the Stefan condition at the liquid–vapor interface. These solutions are often used in the literature to validate numerical phase-change models. Subsequently, numerous studies have been proposed for the estimation of wall condensation phenomena, both through a correlation-based approach [10–14] and by modeling the interface using CFD techniques [15–17]. The latter, predominantly developed in Volume of Fluid (VOF) environment, are mostly based on defining source terms at the interface, primarily governed by kinetic gas theory and non-equilibrium models [18], as well as enforcing the heat flux balance and saturation temperature conditions at the interface [15]. While empirical approaches suffer from uncertainties and limitations in the range of applicability, the CFD approach can lead to high computational costs due to the need to model the thermal and dynamic boundary layers at the interface. It is evident that such a computational effort is incompatible with the long characteristic times required to capture the entire thermal transient of the machine.

In the context of phase change in steam turbines, where wall condensation occurs in ducts with predominantly horizontal development, it is easily verifiable using film flow regime maps proposed in the literature (e.g., Tandon et al. [19]) that the prevailing flow regime is stratified, consisting of the formation of a laminar film in the upper part of the duct. Leveraging this information, this article proposes and validates a simplified multiphase model for the simulation of a laminar film flow regime. The goal is to overcome the prohibitive computational costs of common interface reconstruction models while maintaining a three-dimensional description of the flow field, which a correlation-based approach would not be able to capture.

Given the previously mentioned coupled nature of the phenomenon, it is evident that its numerical simulation must necessarily account for the conjugate solution of the flow field and the energy equation in the fluid domain. For this type of problem, maintaining temporal consistency between the two solvers is crucial. The primary challenge to consider is the significant disparity in characteristic timescales typically present in such applications, as highlighted by He [20]. In particular, He and Fadl [21] have shown that, from a temporal discretization perspective in a time marching problem, the bottleneck in advancing the solution lies in selecting the smallest time-step for the time marching of the monolithic solution. It is clear that this disparity in characteristic timescales quickly leads to prohibitive computational costs for simulating the entire turbine transient, which generally lasts on the order of several minutes, as shown by Rafanelli et al. [22].

Over the years, numerous numerical methods have been proposed to reduce computational costs, many of which are based on the so-called loosely coupled quasi-steady approach (Gimenez et al. [23] and many others). This approach relies on the strong disparity between the characteristic timescales of transport mechanisms in the fluid domain compared to conduction in the solid. In this case, if such a disparity is verified, the fluid domain exhibits an almost instantaneous response to wall temperature variations, making the time derivative term of fluid equations negligible. This allows solving the fluid system using a steady-state approach while enforcing temperature and heat flux continuity at the wall interface with a time-step several orders of magnitude larger than what a fully coupled monolithic CHT solution would require.

Another widely used method in the literature to reduce computational costs associated with the disparity of characteristic timescales is the so-called Fourier number (Fo) scaling method (Shi et al. [24] and many others), which is based on scaling down the thermal diffusivity by a fixed scaling factor.

While these two methods are highly effective in achieving their goal, successfully cutting computational costs by up to three orders of magnitude, they are still subject to the stringent assumption of a strong disparity in characteristic timescales, which is not always verified. Fadl and He [25] simulated a natural convection problem in the context of steam turbine cooling following machine shutdown, demonstrating the unreliability of the quasi-steady method for this transport mechanism. For this reason, the loosely coupled Dual time-step method has been proposed to account for the temporal history of the solution by introducing appropriate source terms in the governing equations. This method has shown excellent predictive capability for thermal transients, even in conditions where the fluid domain's temporal history is no longer negligible. Additionally, it has demonstrated stability in the solution, even with time-steps larger than those permitted by a fully coupled CHT approach.

In the problem of wall condensation, in addition to the convective transport of the vapor itself, the convective transport of a condensate film with trivial thermo-fluid dynamic characteristics is present. In particular, it shows typically very low velocities, extremely thin thickness, and thermal diffusivities similar to solid ones. In this work, after estimating the disparity in characteristic timescales of the transport mechanisms involved, the previously mentioned computational cost reduction methods are applied. The advantages and limitations of each approach in accurately simulating a wall condensation problem are highlighted.

2. Multiphase model and benchmark monolithic solution

The validation data were obtained from a benchmark transient wall condensation simulation using a strongly coupled approach, with a time-step ensuring the stability of the fluid solution. This chapter presents the computational domain used in the simulation, the models employed, and the boundary conditions.

2.1. Computational domain and boundary conditions

The simulation has been carried out with ANSYS Fluent code, the computational domain for the transient multiphysics simulation is shown in Fig. 1.

It is a vertical flat plate with length $L = 0.5\,\mathrm{m}$,thickness $s = 0.005\,\mathrm{m}$ and depth $W = 0.1\,\mathrm{m}$, exposed to a flow of saturated vapor in the same direction as the gravitational acceleration. The transient simulation is

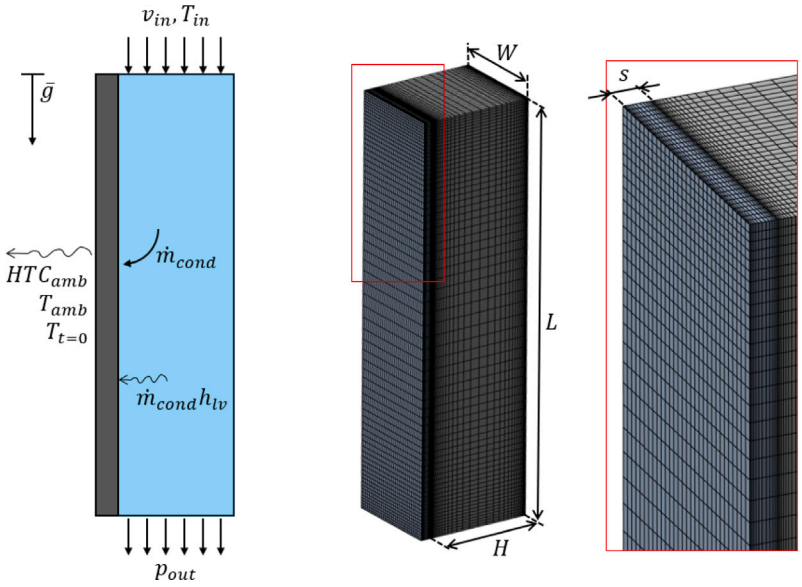

Fig. 1. Computational domain of the vertical flat plate.

initialized at a temperature $T_{t=0}$ below the saturation level. As shown in Fig. 1, the left side is subjected to a convection condition with the environment, with an imposed HTC_{amb} and T_{amb} while the right side experiences heat release due to wall condensation. The grid generated for the described domain is shown on the right side of Fig. 1 and consists of a structured mesh of approximately 100,000 hexahedral cells. The geometric data, initial conditions, and boundary conditions of the simulation are summarized in Table, where λ, c and ρ are respectively the heat conductance, the specific heat and the density, while the subscript s refers to the plate material.

Variable	Value	Unit
v_{in}	10	[m/s]
T_{in}	373.15	[K]
T_{amb}	293.15	[K]
$T_{t=0}$	300	[K]
HTC_{amb}	20	[W/m^{2}K]
p_{out}	1	[atm]
λ_s	20	[W/mK]
c_s	500	[J/kgK]
ρ_s	5000	[kg/m^3]

The analysis involves the solution of the Reynolds-averaged Navier–Stokes equations with the two-equation $k-\omega\,SST$ model for turbulent diffusivity calculation of the vapor domain for which computational grid has been built to maintain wall y+ around unity, and only the heat equation with transient and diffusive terms for the flat plate. For a fully coupled CHT (Conjugate Heat Transfer) problem, the following continuity conditions for temperature and heat flux are imposed at the fluid–solid interface at each iteration:

$$T_f = T_s \tag{1a}$$

$$-\lambda_f \frac{\partial T_f}{\partial n} = -\lambda_s \frac{\partial T_s}{\partial n} \tag{1b}$$

In the next paragraph, the multiphase model proposed for the simulation of wall phase change is presented and validated with two benchmark analytical solutions, both widely used in literature for wall phase change models validation, and with experimental data of axial distribution of laminar condensing film heat transfer coefficient.

2.2. Multiphase model: description and validation

Given the laminar nature exhibited by a film in a stratified regime, Fluent's built-in model "Eulerian Wall Films" was chosen for its good balance between computational cost and result accuracy, as previously demonstrated in literature [26,27]. The model solves mass, momentum, and energy transport equations in the 2D wall domain at the fluid-plate interface in the following form:

$$\frac{\partial(\rho_l \delta)}{\partial t} + \nabla \cdot (\rho_l \mathbf{u} \delta) = S_\rho \tag{2a}$$

$$\frac{\partial(\rho_l \delta \mathbf{u})}{\partial t} + \nabla \cdot (\rho_l \mathbf{u}\mathbf{u} \delta + D_\mathbf{u}) = S_\mathbf{u} \tag{2b}$$

$$\frac{\partial(\rho_l \delta T)}{\partial t} + \nabla \cdot (\rho_l \mathbf{u} T \delta + D_T) = S_T \tag{2c}$$

where the source terms on the RHS of the equations represent phase change mass flux (Eq. (2a)), vapor shear stresses, vapor pressure, film spreading, gravity force, surface tension (Eq. (2b)), heat flux and phase change heat release (Eq. (2c)).

Due to the lack of a built-in model that describes condensation mass flux based on the temperature gradient, an equilibrium phase-change model based on the Stefan condition at the interface was implemented via a C language based User-Defined Function (UDF). This equilibrium approach, widely used in the literature, especially in Volume of Fluid (VOF) environments [15,17], turns out to be capable to predict the interface condensation with low interface dynamics. For accurate mass flux estimation, as highlighted by Szijarto [17], it is essential to estimate the temperature gradients at both the vapor and liquid sides of the interface. The condensation mass flux formulation with the absence of radiation effect in a phase equilibrium model can be derived as follows [17]:

$$\dot{m}_{lv} = \frac{\lambda_v \left.\frac{\partial T_v}{\partial n}\right|_{if} - \lambda_l \left.\frac{\partial T_l}{\partial n}\right|_{if}}{h_{lv}} \tag{3}$$

where on the RHS the temperature gradients are written for both phases at the interface. In this case, while the temperature gradient of the vapor can be directly extracted from the solution of the thermal boundary layer, the calculation of the liquid temperature gradient is greatly simplified by the laminar conditions of the film. The heat flux balance based phase-change model can therefore be summarized in the

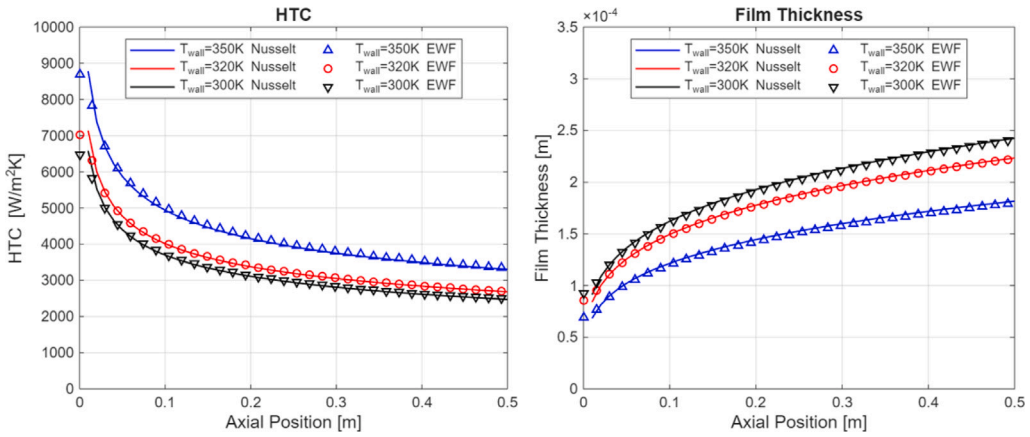

Fig. 2. Comparison between phase change model results and Nusselt benchmark solution of heat transfer coefficient (left) and film thickness (right) at three different temperature imposed at wall.

following source terms:

$$S_\rho = \frac{\lambda_v \nabla T_{v,n} - 2\lambda_l (T_{sat} - T_{\delta/2})/\delta}{h_{lv}} \tag{4a}$$

$$S_T = S_\rho h_{lv} \tag{4b}$$

where h_{lv} is the latent heat, the subscript n is the normal direction to wall and the half depth film temperature $T_{\delta/2}$ is computed directly from the solution of Eq. (2c).

As an intermediate step, the model was validated against the steady-state analytical solution of Nusselt [8], which describes the spatial evolution of the film thickness and the heat transfer coefficient along a vertical flat plate at constant temperature in the absence of shear stresses at the interface. The analytical formulation for the film thickness and HTC along the flat plate is as follows:

$$\delta(x) = \left[\frac{4\mu_l \lambda_l (T_{sat} - T_{wall})x}{g\rho_l(\rho_l - \rho_v)h_{lv}}\right]^{0.25} \tag{5a}$$

$$HTC(x) = \left[\frac{g\rho_l(\rho_l - \rho_v)h_{lv}\lambda_l^3}{4\mu_l(T_{sat} - T_{wall})x}\right]^{0.25} \tag{5b}$$

The boundary conditions for the validation are ambient pressure and three constant wall temperature conditions of 300K, 320K, and 350K, with a saturation temperature of 373.15K. In Fig. 2, a comparison is shown between the analytical solution and the one predicted by the Eulerian film model for the film thickness (right) and the heat transfer coefficient (left). The results show a remarkable agreement with the analytical solution, indicating a correct prediction of the steady flow field and the temperature gradient across the film within the analyzed wall temperature range.

Dealing with a transient problem, the model has also been validated with the analytical solution of the Stefan problem [9], which describes the 1D temporal evolution of the thickness of a quiescent liquid layer formed by phase change. The governing equation of the problem is the one-dimensional heat equation with appropriate energy jump conditions at the interface:

$$\frac{\partial T}{\partial t} = \frac{\lambda_l}{\rho_l c_{p,l}} \frac{\partial^2 T}{\partial x^2} \qquad 0 \le x \le \delta(t) \tag{6a}$$

$$\rho_l v_\delta h_{lv} = -\lambda_l \frac{\partial T}{\partial n}\Big|_{x=\delta(t)} \tag{6b}$$

where $\delta(t)$ is the time dependent interface position and v_δ represent its velocity. The temperature boundary conditions are:

$$T(x = 0, t) = T_w \tag{7a}$$

$$T(x = \delta(t), t) = T_{sat} \tag{7b}$$

The exact time dependent position of the interface can be determined following Stefan problem analytical solution [9] at can be written as follows:

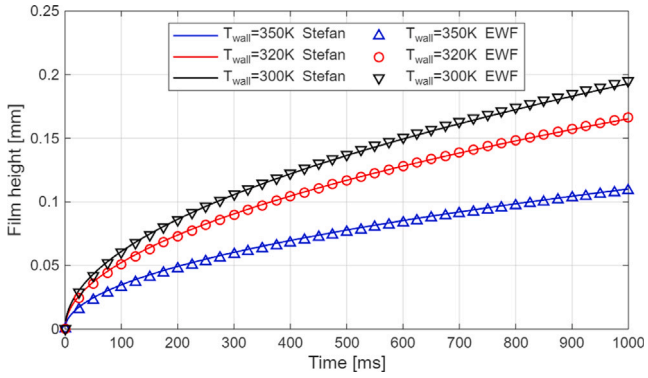

Fig. 3. Comparison between phase change model film thickness prediction and analytical solution of 1D Stefan problem with three different imposed wall temperature.

$$\delta(t) = 2\chi\sqrt{\frac{\lambda_l t}{\rho_l c_{p,l}}} \tag{8}$$

where χ is the solution of the following trascendental equation:

$$\chi exp(\chi^2) erf(\chi) = \frac{c_{p,l}(T_{sat} - T_w)}{h_{lv}\sqrt{\pi}} \tag{9}$$

In Fig. 3, the comparison between the numerical result and the analytical solution of the Stefan problem is shown, with a fixed wall temperature of 300K, 320K, and 350K, and a saturation temperature of 373.15K.

The agreement shown in Fig. 3 indicates a correct imposition of the energy jump at the interface, a condition that is intrinsically linked to the calculation of the phase change flow rate. The excellent agreement with the analytical solutions, both steady-state and transient, makes this model suitable for the prediction of the equilibrium-based enthalpy jump across the interface, which is essential to predict the phase change rate.

Finally, the validation against experimental data is carried out in order to assess its reliability in real applications. For this purpose, the test case developed by Lee [28] was selected, specifically designed to investigate the heat transfer coefficient for laminar filmwise condensation under different operating conditions. The experimental apparatus consists of a 304 stainless steel vertical circular tube with an internal diameter of 0.013 m and a length of 2.8 m, into which saturated steam is injected downward. The outer surface of the tube is cooled by a

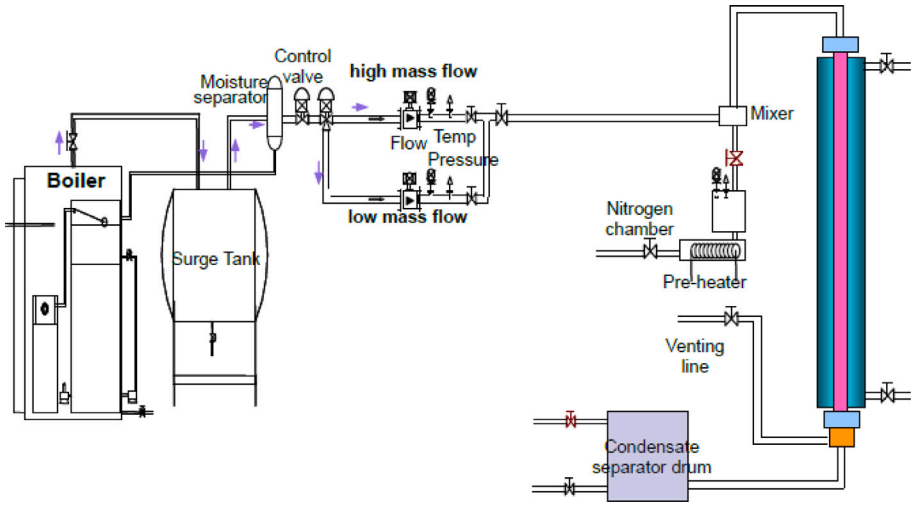

Fig. 4. Experimental apparatus of Lee [28] experiment.

Table 1
Operating conditions selected for validation [28].

Case	D_i [m]	T_{sat} [°C]	p [kPa]	$\dot{m}_{vap}$ [kg/s]
Lee1	0.013	100.84	104.5	0.006106
Lee2	0.013	102.74	110.7	0.007836

upward of water. The experimental apparatus developed by Lee [28] is shown in Fig. 4.

Although this test case was originally developed to study the effect of non-condensable gases, within the wide set of experimental data there are also cases with pure steam at the inlet. Due to the small tube diameter, under operating conditions where the steam mass flow rate is not sufficiently high, complete condensation of the steam flow occurs, leading to a null quality of the inlet mixture. Because of the two-dimensional nature of the model, only the operating conditions where complete condensation of the steam does not occur along the tube, and obviously in the absence of non-condensable gases, were selected for validation purposes. The selected operating conditions are reported in Table 1.

Given the strong coupling between the wall temperature field and the flow field of the laminar condensate film, a steady-state CHT simulation was performed by simultaneously solving the three domains of vapor, tube wall, and cooling water. This approach avoided the use of empirical correlations for the cooling side, which would have introduced additional uncertainty into the results. Due to the high aspect ratio of the domain (0.013 m diameter, 2.8 m length), the circumferential invariance of the experimental results [28] was exploited to simulate only a 90° sector of the domain, leading to a significant reduction in computational cost. Overall, the mesh consisted of approximately 12 million tetrahedral elements, and the simulations were carried out using the ANSYS Fluent solver. The comparison between experimental data and prediction of axial Heat Transfer Coefficient by the proposed model is reported in Fig. 5.

Given the high aspect ratio of the domain, the global film thickness contour would have been unreadable. For this reason, Fig. 6 reports the contour in the vicinity of the vapor inlet, where the trend of the film thickness (result of film continuity equation) along the inner wall of the tube is visible, together with the coolant and plate temperature distribution plotted on the outlet surface and on the periodic boundaries of the 90° sector.

The good agreement shown in Fig. 5 confirms the capability of an equilibrium phase-change model applied at the free surface of a lubrication-regime film to predict its heat transfer performance due to wall condensation.

Once the capability of correctly predicting the interfacial enthalpy jump, both in steady and transient ideal conditions, and of reproducing the heat transfer performance under real operating conditions has been confirmed, the analysis proceeds with the investigation of the model behavior coupled with a time dependent interface temperature due to the thermal transient of the solid plate. The next section is therefore dedicated to the transient CHT simulation of the phenomenon under study, first with a monolithic approach, which is computationally demanding but ensures temporal consistency at each iteration across the coupled domains, and then by exploring several computational cost reduction techniques proposed in the literature. The advantages and limitations of each approach for the problem of wall condensation are finally discussed.

2.3. Results of the reference monolithic analysis

This section presents the results obtained from the reference transient fully coupled CHT simulation. For this analysis, 8 CPUs were used for the parallel computation of approximately 40000 time-steps, with a time-step size of $5 * 10^{-4}$ s, resulting in a total computation time of around 12 days. It is worth mentioning that, for a real geometry, this time could be further extended due to the extreme simplicity of the domain and the reduced thickness of the flat plate used in this simulation, which inevitably reduces the characteristic time of energy diffusion. As highlighted by Rafanelli [22], the transient of a real turbine can last several tens of minutes, which is at least one order of magnitude longer than what was analyzed in this work. The post-processing of the results shown in Fig. 7 includes the wall temperature monitor at two points across the thickness of the flat plate (red dots) and the film thickness at two points along the plate (blue dots).

The Fig. 8 shows the temperature results (left) and film thickness (right) at the points referenced in Fig. 7.

As already mentioned, it is observed that the initial solution of the fluid domain and the Eulerian film refer to the steady-state solution linked to the initial wall temperature. From the results, it is evident that as the energy solution progresses, the temperature at the interface between the domains rapidly increases, thereby reducing the temperature gradient across the film, and consequently, reducing the condensate flow rate. This, in turn, leads to a gradual reduction in the film thickness. It is therefore clear that the correct prediction of the temperature cannot be separated from the correct estimation of the film's flow field, and vice versa. These data are used as a benchmark for the validation of the multiphysics approaches aimed at reducing computational cost, which are proposed in the next paragraph.

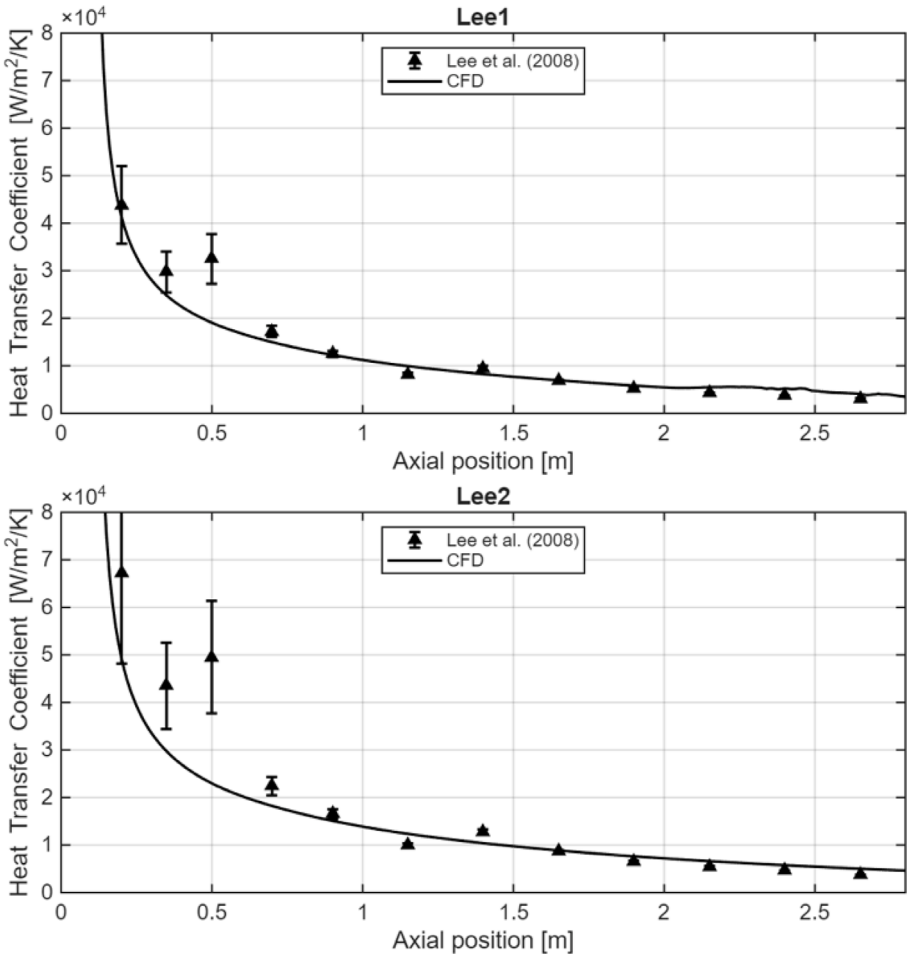

Fig. 5. Comparison with experimental data from [28]: Lee1 (above) and Lee2 (below) operating conditions.

3. Numerical methodology: cost reduction techniques

The following multiphysics approaches, after being briefly introduced, are implemented for the case under examination:

- Quasi-steady (QS) approach: loosely coupled multiphysics method in which fluid equations are solved in a steady framework.
- Fourier number scaling method: fully coupled method based on the solid thermal diffusivity reduction.
- Dual time-step (DTS) method: source terms based loosely coupled method which externally predicts the time derivative term in a steady framework.

The simulations conducted in this work were performed using ANSYS Fluent software, employing C language-based User Defined Functions (UDFs) to manage the fluid–solid interface for the loosely coupled methods, to define source terms in the Dual time-step model, and to store information in User Defined Memory (UDM) in the Dual time-step model.

3.1. Costs reduction techniques: Quasi-steady approach

The significant difference in characteristic times of the transport mechanisms typically occurring in turbomachinery applications (He et al. [20]) has often led to the use of quasi-steady approach for transient CHT simulation of the machine components themselves [23,29]. In particular, given the short characteristic time related to fluid convective transport, the hypothesis behind this method is that the fluid domain's response is instantaneous to the temperature change caused by conduction in the solid. This hypothesis allows decoupling from the transient solution of the solid domain, thereby eliminating the bottleneck of the time-step constraint required to avoid stability issues. In this case, the advancement of the solid domain can occur with a time-step typical of conductive transport, several orders of magnitude larger than the one required for the fluid domain's time marching. The standard implementation of this approach is reported in Fig. 9.

This procedure can be summarized in the following steps:

1. Time marching of solid domain with a large sized time-step
2. Either temperature (Dirichlet) or heat flux (Neumann) condition passed to fluid interface
3. Run of a steady-state fluid simulation with updated boundary conditions
4. HTC and T_{bulk} (Robin) condition passed back to the solid
5. Convergence check: if not satisfied, step back to point 1; if satisfied, further marching of the solid solution

This is essentially a time history of the fluid domain without memory, which responds instantaneously to the thermal history of the solid. It is worth mentioning that, the less pronounced the disparity in characteristic times of the transport phenomena, the less valid this hypothesis will be.

3.2. Costs reduction techniques: Fourier number scaling method

The thermal diffusivity scaling method has been widely used in the literature due to its straightforward implementation. As highlighted by Shi et al. [24], since in the dimensionless conduction equation the

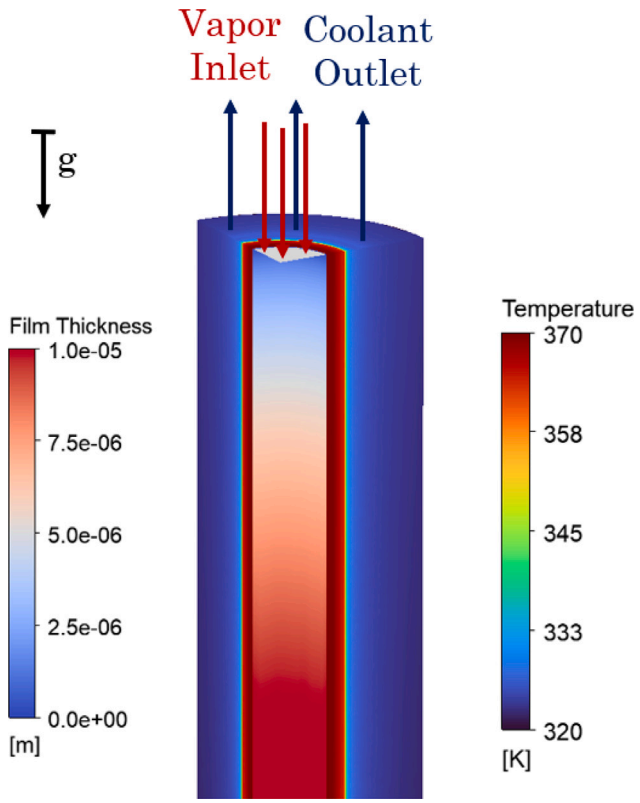

Fig. 6. Contours of: film thickness along the inner surface of the tube; coolant and tube temperature on the periodicity and upper surface of the domain.

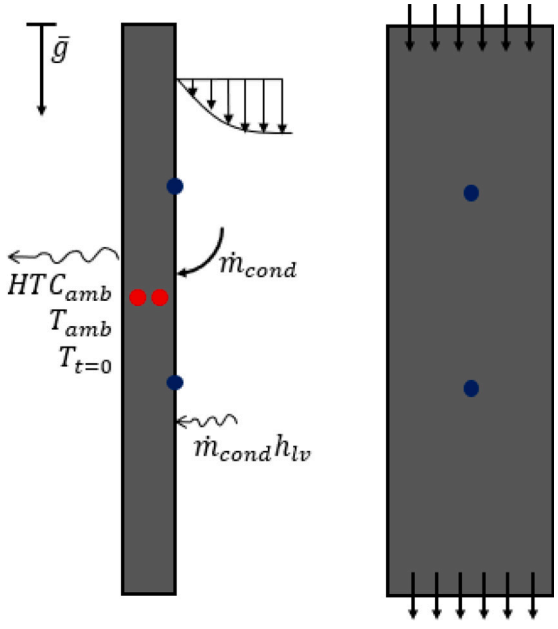

Fig. 7. Post-processing locations for temperature probes (1=right red dot; 2=left red dot) and film thickness probes (1=upstream blue dot; 2=downstream blue dot).

time variable is replaced by the Fourier number, reducing the heat capacity $\rho_s c_s$ of the solid material by a factor of N results in a temporal advancement amplified by the same factor N while maintaining the same steady solution (not changing the Biot number). This allows maintaining a fully coupled transient framework, preserving a time-step that ensures the stable solution of the fluid equations while compressing the characteristic time of the solid domain. In turbomachinery applications, this method has demonstrated significant advantages, yielding results consistent with the original monolithic solution for Fourier number reduction factors of up to 10^3. For the reasons mentioned above, this reduction directly translates into a substantial decrease in computational cost by the Fourier number reduction factor itself.

3.3. Costs reduction techniques: Dual time-step method

The Dual time-step method, proposed by He and Fadl [21] and applied by Fadl and He [25] for a natural convection problem, is based on the introduction of a source term for each equation solved in the fluid domain within a steady-state framework. Considering the generic time dependent variable Φ, the source term takes the following second-order backward implicit form:

$$S_{\Phi} = \frac{1.5\Phi^{M,k} - 2\Phi^{M-1} + 0.5\Phi^{M-2}}{\Delta t} \tag{10}$$

where M is the current time-step, k is the current sub-iteration of the relative time-step and Δt is the physical time-step. The equations of the fluid domain involved in the simulation under consideration become the following:

$$\frac{\partial \mathbf{U}}{\partial \bar{t}} + R(\mathbf{U}) = S_{\mathbf{U}} - \left(\frac{1.5\mathbf{U}^{M,k} - 2\mathbf{U}^{M-1} + 0.5\mathbf{U}^{M-2}}{\Delta t}\right)_{UDF} \tag{11a}$$

$$\frac{\partial \mathbf{U}_F}{\partial \bar{t}} + R(\mathbf{U}_F) = S_{\mathbf{U}_F} - \left(\frac{1.5\mathbf{U}_F^{M,k} - 2\mathbf{U}_F^{M-1} + 0.5\mathbf{U}_F^{M-2}}{\Delta t}\right)_{UDF} \tag{11b}$$

where $\bar{t}$ is the pseudo time linked to the steady solution, $(\mathbf{U})$ is the vector containing the 3D domain conservative variables $(\rho, \rho u, \rho v, \rho w, \rho E, \rho k, \rho\omega)$ and the components of vector $(\mathbf{U_F})$ are the 2D film variables $(\rho_l\delta, \rho_l\delta u_F, \rho_l\delta v_F, \rho_l\delta T_F)$ resolved in the fluid–solid interface domain.

The vanishing of the first term on the LHS due to the steady-state solution thus leads to obtaining the time derivative term with the formulation presented in Eq. (10). Storing the variables at previous time-steps allows for the calculation of a time derivative that accounts for any potential inertia in the transport within the fluid domain. Fadl and He [25] demonstrated that calculating the time derivative with an implicit scheme makes the solution unconditionally stable, enabling advancement in the solution with typical time-steps for heat diffusion in the metal, while still quantifying the thermal inertia of the fluid solution, which can sometimes show up. For a deeper understanding of this approach, the reader is referred to the reference article.

To ensure the continuity of temperature and heat flux at the interface in loosely coupled simulations, the approach of [25] was followed. In this approach, to correctly discretize the time advancement in the solid domain, the term of the form (10) was added to the plate energy equation, leading to the following formulation of the transient heat conduction:

$$\frac{\partial T}{\partial \bar{t}} + R(T) = -\left(\frac{1.5T^{M,k} - 2T^{M-1} + 0.5T^{M-2}}{\Delta t}\right)_{UDF} \tag{12}$$

This allows temporal advancement in the solid solution while remaining within a steady-state framework. Therefore, for loosely coupled simulations, the temporal framework of both solvers is of steady-state type, allowing a steady "pseudo-monolithic" solution approach, in which temperature and heat flux continuity is enforced at each iteration by the solver.

4. Results and discussion

This section presents the results related to the approaches commonly used to reduce the computational cost in solving long transient problems, highlighting the advantages and limitations of each method.

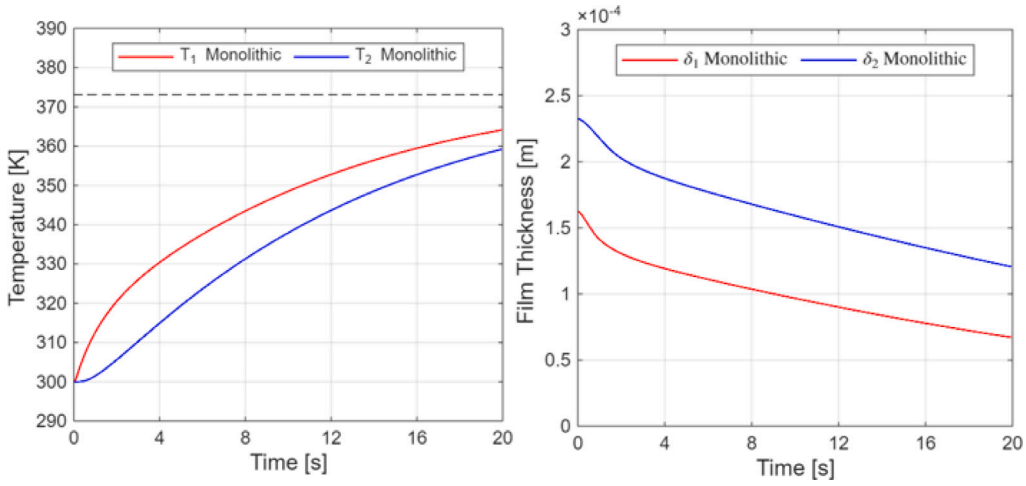

Fig. 8. Results of reference monolithic simulation in terms of plate temperature (left) and film thickness (right).

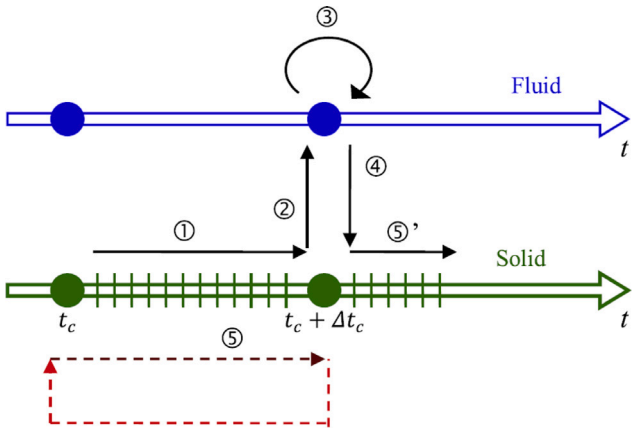

Fig. 9. Coupling strategy from Gimenez [23].

4.1. Results of cost reduction techniques: comparison with benchmark monolithic solution

4.1.1. Quasi-steady approach

The quasi-steady method has been implemented in Fluent code and applied to the flat plate model under examination, and the results in terms of thermal history and film thickness are shown in Fig. 10. For this simulation, for the solid time marching, a time-step of 50 ms was chosen (100 times larger than the fluid time-step chosen previously), and the coupling between the solutions was performed at each time-step of the solid solution. In this coupling, the continuity condition of temperature and heat flux was imposed.

From the comparison shown in Fig. 10, a slight under-prediction of the film thickness during the initial part of the transient can be observed, which inevitably leads to an overestimation of the heat transfer coefficient and, consequently, an average temperature overestimation throughout the entire transient. Although this is not a significant underestimation (around 6% in terms of film thickness), it is certainly an unacceptable result even in light of substantial computational savings. To explain this underprediction, it is useful to quantify the characteristic times of the transport phenomena involved in this specific case. Following the procedure of He [20], the disparity in characteristic times between fluid convective transport and diffusion in the solid can be quantified as follows:

$$\frac{\tau_s}{\tau_f} = \left(\frac{c_{ps}}{c_{pf}}\right)\left(\frac{\rho_s}{\rho_f}\right)\left(\frac{\lambda_f}{\lambda_s}\right)\left(\frac{s}{L}\right)^2 Pr_f Re_f \tag{13}$$

By substituting the vapor thermodynamic properties and the boundary conditions of the problem, the vapor/plate disparity in characteristic time settles in the order of 10^4. This value aligns with what is observed in the literature, confirming the hypothesis of the vapor's instantaneous response. Considering the convective transport of the film, imposing the thermo-fluid dynamics conditions resulting from the steady-state solution, a film/plate characteristic time disparity of the order of 10^0 is found, primarily due to a significantly lower density ratio and a Reynolds number limited by the reduced thickness that a laminar film of this type typically presents.

With reference to the film continuity described in Eq. (2a), Fig. 11 shows the time evolution of the three terms that compose it in the monolithic simulation. It can be observed that, in this case, the characteristic times similarity between film convective transport and plate diffusion does not allow the time derivative term from being considered negligible, making the quasi-steady assumption no longer verified. As a consequence, it can be seen from Fig. 10 on the right that the thickness obtained from the quasi-steady simulation is unable to reproduce the inflection point present after about 1 s from the start, caused by the no longer negligible inertia of the film. This initial underestimation of the thickness is due to the presence of the maximum of the time derivative term shown in Fig. 11.

It is worth mentioning that these results are specific to the chosen material and fluid dynamic conditions and should not be regarded as absolute truth. From a general point of view, by examining Eq. (13), the following considerations can be made regarding the error introduced by the quasi-steady approach:

- With a plate with lower thermal diffusivity (e.g. aluminum, copper), the error would increase.
- With a thicker plate, the error would decrease.
- In a real geometry, where the development is not exclusively vertical, the gravity driving force would generally be lower, leading to Reynolds numbers even lower than those found for the vertical flat plate. Consequently, the convective transport of the film would be even slower, and the error of the quasi-steady approximation would increase.

4.1.2. Fourier-scaling method

The scaling of the heat capacity has been applied to the case under examination, selecting a heat capacity reduction factor of $N = 10$ and $N = 100$, equivalent to an accelerated time marching in the heat equation solution by the same factor. In this case, as previously mentioned, the simulation framework is transient, and the interface management between the domains is fully coupled, as in the monolithic simulation.

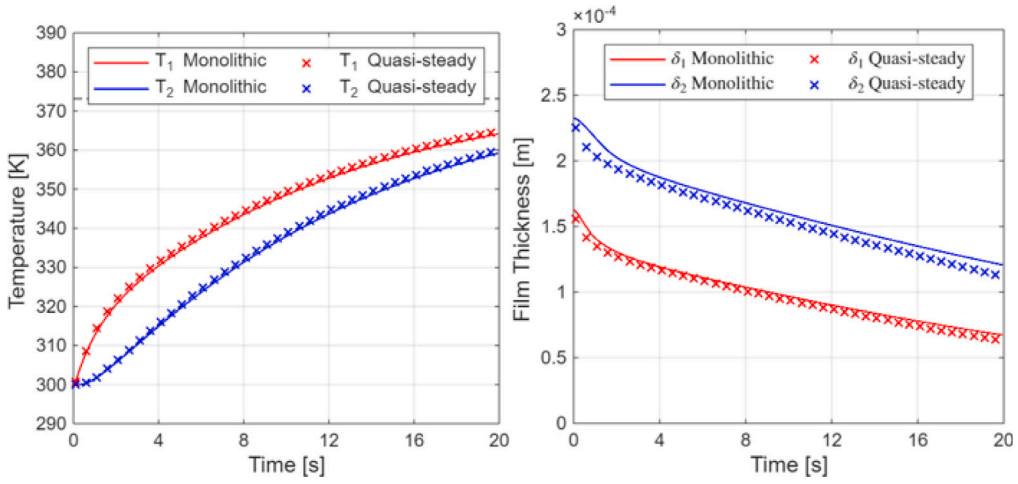

Fig. 10. Comparison between results of monolithic solution and simulation with quasi-steady approach in terms of plate temperature (left) and film thickness (right).

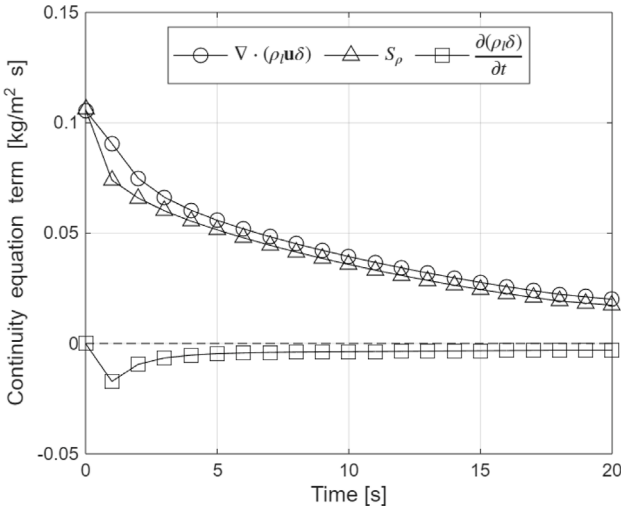

Fig. 11. Film continuity equation terms transient behavior.

Fig. 12 shows the results in terms of film thickness and metal temperature for the cases $N = 10$ (dashed line) and $N = 100$ (dash–dot line). From the plots, it can be observed that the model is entirely incapable of predicting the behavior of the film, the heat transfer coefficient, and consequently, the metal temperature, leading to unacceptable results.

The inadequacy of the model can be attributed to the coupling between the heat equation in the solid domain and the film continuity equation. In this model, since the solution of the heat equation is accelerated by a factor of N due to the reduction of the heat capacity by the same factor, it effectively lead the wall temperature to advance in time N times faster:

$$T_w = T_w(x,t) \xrightarrow{Fo-scaling} T_w = T_w(x,Nt) \tag{14}$$

Since it is still a fully transient framework, the time-step used to advance the solution of the film equations remains the initial one. Given that the term on the right-hand side of the film continuity equation (condensation rate) is highly dependent on the temperature gradient across the film itself and, by extension, on the wall temperature, it can be assumed that the condensation source term advances along with the solution of the solid domain:

$$\dot{m}_{cond} = \dot{m}_{cond}(x,T_w(t)) \xrightarrow{Fo-scaling} \dot{m}_{cond} = \dot{m}_{cond}(x,T_w(Nt)) \tag{15}$$

hence obtaining the following formulation of film continuity equation:

$$\frac{\partial(\rho_l\delta)}{\partial t} + \nabla\cdot(\rho_l \mathbf{u}\delta) = \dot{m}_{cond}(x,T_w(Nt)) \tag{16}$$

Due to the presence of the time derivative term, an inconsistency arises between the temporal advancement of the source term (advancing *"N times faster"*) and that of the film solution itself (advancing *"one time faster"*). On the other hand, if the quasi-steady fluid condition were satisfied and the time derivative term were nearly zero, the transient term would no longer have any influence, and the steady-state solution of the film would advance together with the transient solution of the solid, to which the condensation rate source term is inherently linked. From this analysis, the following conclusion can be drawn: the Fourier number scaling procedure is valid only under the assumption of very low inertia and a negligible time derivative in the fluid domain. Those hypothesis are basically the same under the quasi-steady approach.

4.1.3. Dual time-step method

In this analysis, Dual time-step method was compared with the monolithic solution by considering the advancement in the solid domain solution with time-steps of 5 ms (10 times the fluid one) and 50 ms (100 times the fluid one). For the sake of clarity, the parameter N, which in Fourier number scaling method where linked to the heat capacity reduction, in loosely coupled methods (both QS and DTS) represents the ratio between the actual time-step in transient solid solution and the previous time-step used for the monolithic simulation. The coupling between the two domains is carried out at each time-step of the solid domain solution, imposing continuity of temperature and heat flux at the interface. Unlike the quasi-steady approach, this method considers the temporal history of the conservative variables by storing them from previous steady-state solutions and defining source terms in reference to Eq. (10).

In Fig. 13, the results are shown in terms of film thickness (right) and metal temperature (left) for $N = 10$ (top) and $N = 100$ (bottom). In this case, overcoming the assumption of the negligibility of the time derivative term through the source term leads to a significant agreement with the data from the monolithic solution, even with physical time-steps 100 times higher than the initial ones. To quantify the effect of the inertia of the 3D vapor domain, a simulation was finally conducted with the DTS approach N=100, with source terms applied only to the film equations, solving the following set of equations:

$$\frac{\partial \mathbf{U}}{\partial \bar{t}} + R(\mathbf{U}) = S_{\mathbf{U}} \tag{17a}$$

$$\frac{\partial \mathbf{U}_F}{\partial \bar{t}} + R(\mathbf{U}_F) = S_{\mathbf{U}_F} - \left(\frac{1.5\mathbf{U}_F^{M,k} - 2\mathbf{U}_F^{M-1} + 0.5\mathbf{U}_F^{M-2}}{\Delta t}\right)_{UDF} \tag{17b}$$

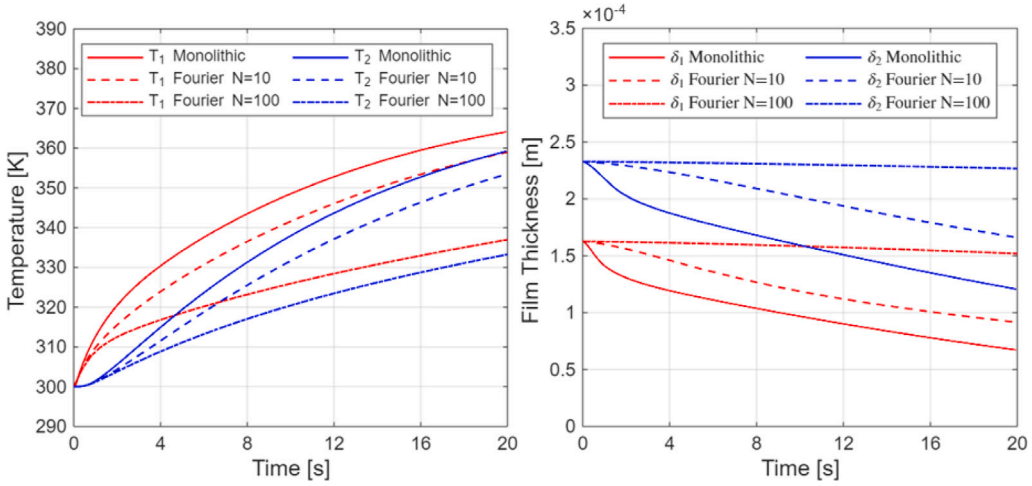

Fig. 12. Comparison between results of monolithic solution and Fourier number scaling method with heat capacity reduction by a factor of 10 (dashed) and 100 (dash–dot) in terms of plate temperature (left) and film thickness (right).

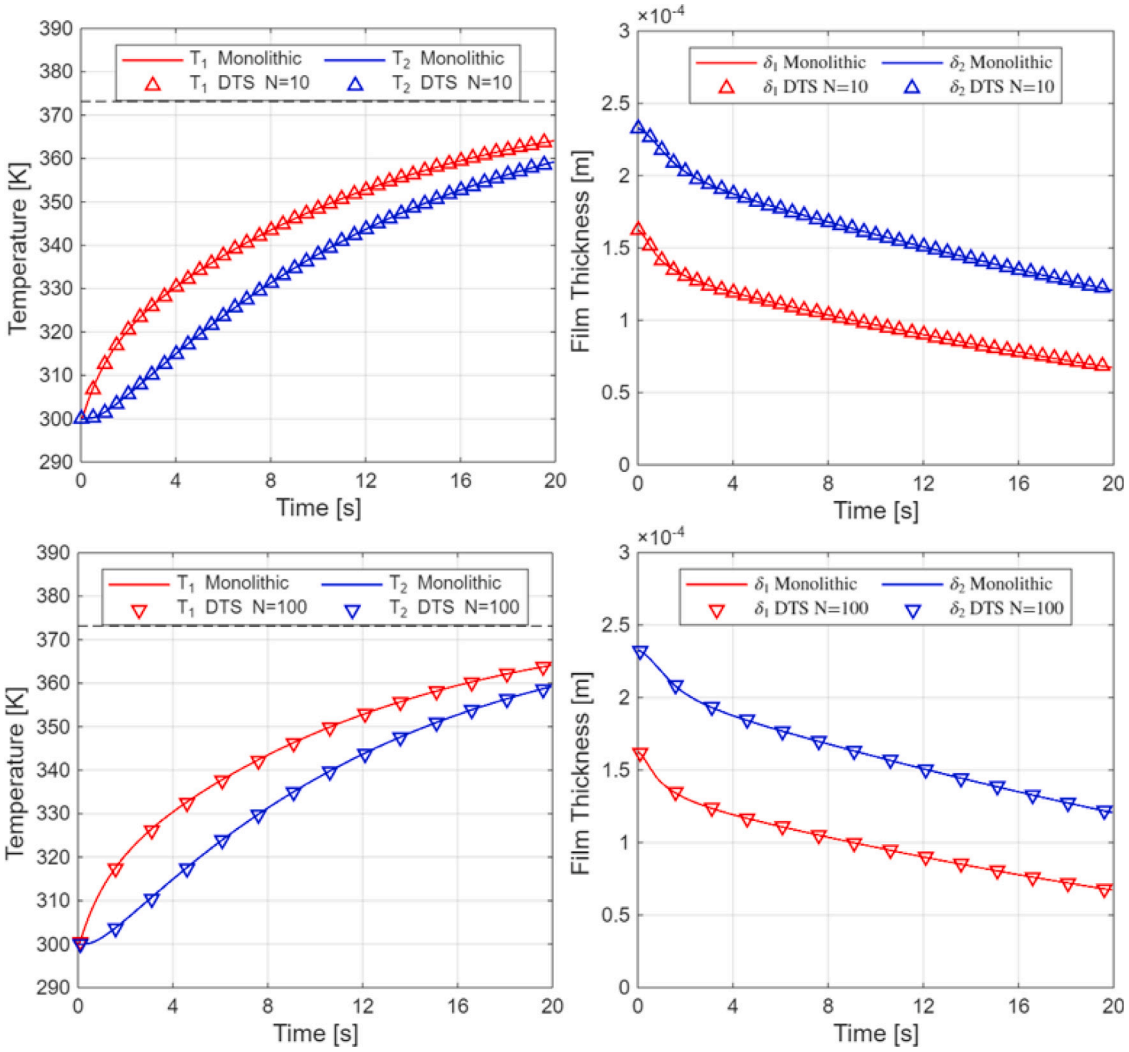

Fig. 13. Comparison between plate temperature (left) and film thickness (right) results of monolithic solution and Dual time-step (DTS) method with time-step of 10 (top) and 100 (bottom) times the one in the monolithic solution.

As shown in Fig. 14, the comparison with the monolithic solution and the agreement with the solution where the source terms are extended to the three-dimensional domain leads to the inevitable and predictable conclusion that the failure of the quasi-steady assumption and Fourier number scaling approach is entirely attributable to the presence of the film, which, as highlighted in the previous chapters,

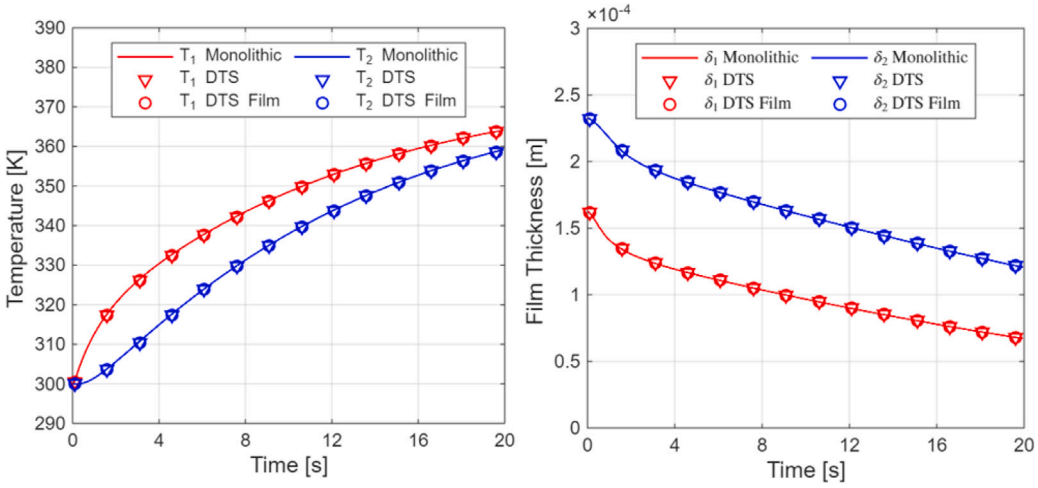

Fig. 14. Comparison between plate temperature (left) and film thickness (right) results of monolithic solution and Dual time-step N=100 with (DTS=triangle) and without (FDTS=circle) the source term on the 3D vapor domain.

exhibits a significantly lower characteristic time disparity than the convective vapor which, in turn, can still be practically considered as without inertia. It is worth mentioning that the computational cost difference between Dual time-step approach with and without the vapor source terms is practically negligible. Therefore, in order to preserve robustness of the model, the DTS approach applied for both 2D liquid film equations and vapor 3D equations is recommended to avoid losing generality and making any assumptions about the characteristic time of any transport mechanism involved in the problem. Obviously, since the domains in which the Eulerian film and the vapor are solved differ in terms of dimensionality (the film is solved at the 2D solid–fluid interface, while the vapor is solved in the 3D domain), the source terms are accordingly formulated to maintain dimensional consistency within their respective domains. In particular, with reference to Eq. (2), it is evident that the source term in the film equations, to be consistent with a 2D domain on which the film is resolved, must be multiplied by the film thickness (see Fig. 14).

4.2. Assessments on vapor side transient behavior

From a transient perspective, it is worth mentioning that in this analysis the boundary conditions for velocity, temperature, and pressure were kept constant over time. Given the transient nature of steam turbine startups, not only from a thermo-structural standpoint but also in terms of thermofluid dynamic inlet conditions to the turbine, the presence of a time dependent boundary condition would lead to a dual scale disparity assessment: between the film and the wall, and between the film and the vapor, due to their mutual dependence. While the former has been successfully investigated in this work, the latter has not been evaluated, as the boundary conditions in the three-dimensional domain were assumed to be steady. In this work, any potential influence of vapor inertia is attributable just to the temporal variation in the mass flow rate removed by wall condensation.

Although this does not fully reflect startup transient conditions, it is worth noting the extensive validation in the literature of quasi-steady approaches for solving the gas-phase domain. As demonstrated by Gimenez et al. [23] and quantified by He [20], in turbomachinery applications there typically exists a strong disparity in characteristic timescales, which makes the quasi-steady assumption between vapor and solid, thus between vapor and film, sufficiently valid. In other words, the short time scales in vapor convective transport mechanisms allows it to adequately recover its steady-state conditions following possible variations at the inlet boundary. However, in the case where such disparity is not present, Fadl and He [25] have shown that the transport inertia of the gas phase can still be successfully captured by the Dual Time-Step method employed in this work. A limitation of its use could arise in the occurrence of periodic boundary conditions with a period shorter than the typical time-step used in the solid domain. In such cases, the temporal advancement of the solution would be unable to adequately discretize the variation in the flow field, leading to inconsistencies and thus inaccuracies in the results. The influence of time dependent boundary conditions and their impact on the film behavior, however, is a little bit beyond the scope of this paper and will be left to future investigations.

4.3. Errors quantification and computational costs comparison

For a clearer overview of the approaches used, the management of the coupling and the main features of the time marching of the models are shown in Fig. 15.

For each model, the spatial and temporal average error in terms of film thickness was evaluated compared to the monolithic solution. The error comparison is shown in Fig. 16.

From the error plot, it can be observed the inadequacy of the quasi-steady model first (with an average error around 5%), and even more so for the Fourier number scaling model (with errors ranging from 15% to 40%), while the Dual time-step method for both $N = 10$ and $N = 100$ show an average error within the order of 0.1%. Finally, it can be noted that the errors for the DTS and FDTS solutions are practically the same, confirming the assumption of a quasi-steady vapor state as predicted by the characteristic times evaluation. In terms of computational cost, although the Fourier number scaling method certainly offers the most effective cost reduction, due to the negligible implementation effort and maintaining the same computational framework, this does not justify the obtained results. Both loosely coupled methods require additional implementation and calculation time, with significantly more encouraging results. In particular, the DTS case for the film only, with N=100, required about 10 h of computation compared to the 12 days required by the monolithic solution. Although this is not a linear scaling with N for the computational cost, it is still an excellent achievement considering the remarkable accuracy of the comparison with reference solution. Fig. 17 presents a summary of the computational time required using the 8 CPUs employed for all simulations.

It is reiterated that, while for loosely coupled simulations (QS, DTS, and FDTS) the scaling factor N refers to the ratio between the solid time-step and the one used in the monolithic simulation, for analyses with the Fourier number scaling approach it refers to the scaling factor of the heat capacity. It can be observed that, for small

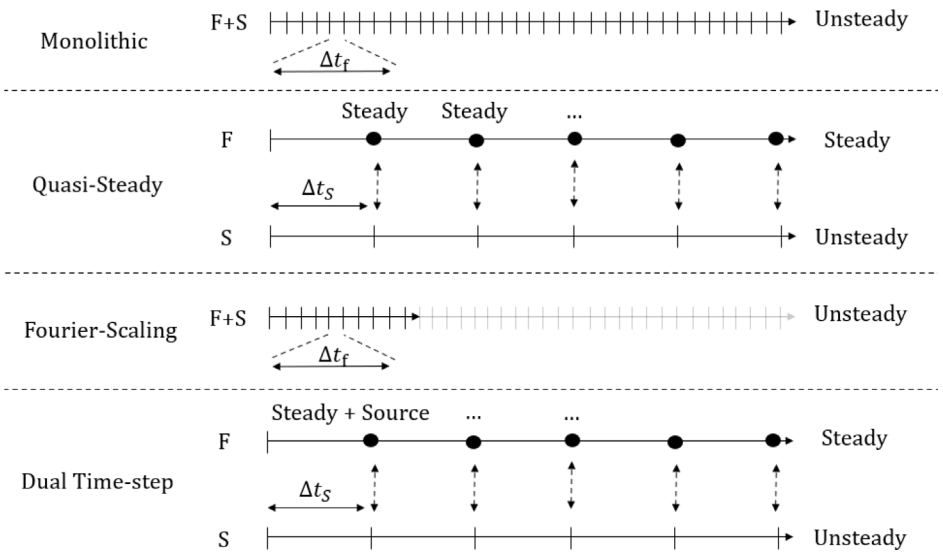

Fig. 15. Fluid–solid coupling and simulation frameworks of the four approaches used in this work.

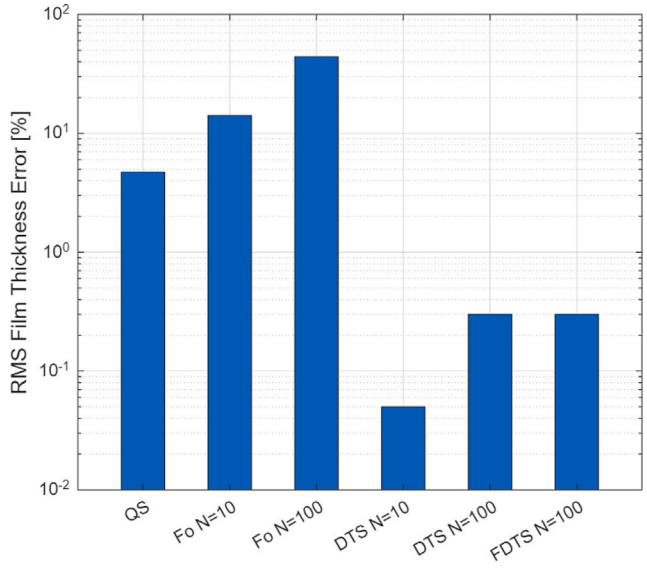

Fig. 16. RMS error (percentage) of the Quasi-steady (QS), Fourier number (Fo) scaling, Dual time-step (DTS) and Film Dual time-step (FDTS) compared to monolithic simulation.

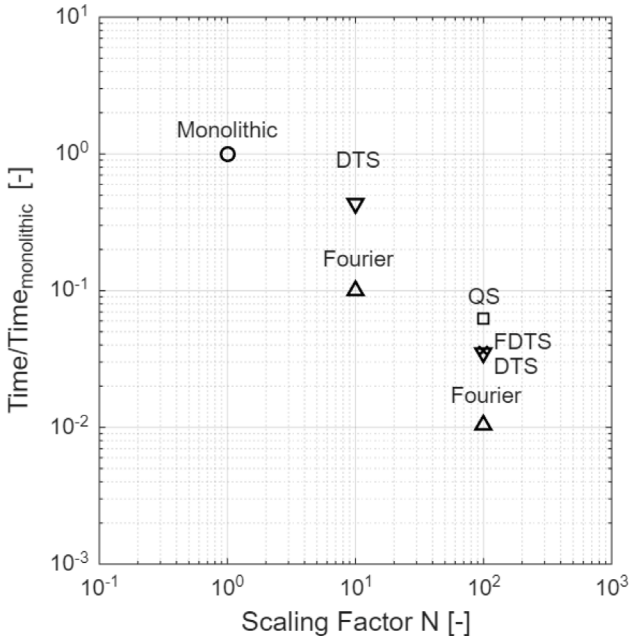

Fig. 17. Simulation time for the analyzed computational saving methods with 8 CPUs compared to benchmark monolithic simulation.

scaling factors, the cutting of computational time is not linear, likely becoming inconvenient for N close to 1. This is mainly due to the higher number of sub-iterations required to solve a steady-state simulation rather than to advance in a time-step. Increasing the scaling factor for loosely coupled simulations provides a real advantage, achieving a considerable 97% reduction in computational time while maintaining excellent agreement with monolithic results in the DTS and FDTS cases. Due to the monolithic nature of simulations using the Fourier number scaling method, the reduction in computational cost is linear with N. However, in this case, the results are entirely unacceptable due to the non-negligible inertia that a thin film inevitably exhibits.

5. Conclusions

With the increasing use of renewable energy sources for Rankine cycles, steam turbines are experiencing more frequent start-ups and shutdowns to cope with the stochastic nature of these sources. Cold start-ups are particularly critical for various aspects of machine design, as they involve high temperature gradients and resulting high stresses, requiring a reliable quantification of the phase change rate to prevent water accumulation during turbine operation.

In this work, a simplified multiphase model for calculating the flow field of a laminar film, typically present in stratified condensate films, was first proposed and successfully validated with both analytical and experimental results. To address the long characteristic timescales typically involved in steam turbine start-up transients, various computational cost-saving approaches have been explored. Based on the results, the following conclusions have been drawn:

(1) The simplified equilibrium-based phase change model has shown remarkable agreement with both analytical solution and experimental data with very low additional implementation and computational costs.

(2) The quasi-steady approach is not suitable because the film exhibits non-negligible inertia due to characteristic transport times similar to those of diffusion in the flat plate.
(3) The Fourier number scaling approach is not applicable as it amplifies the error caused by a non-negligible time derivative term, leading to even more unacceptable results than the quasi-steady approach.
(4) The Dual time-step approach has demonstrated a remarkable ability to predict the temporal evolution of the film and wall temperature, with an average error on the order of 0.1% compared to the reference monolithic solution.
(5) Since the Dual time-step and Film Dual time-step solutions are equivalent, the inapplicability of the quasi-steady approach is entirely attributable to the presence of the thin film.

Nomenclature

Acronyms

CFD	Computational Fluid Dynamics
CHT	Conjugate Heat Transfer
FDTS	Film Dual Time-Step
HTC	Heat Transfer Coefficient
QS	Quasi-Steady
RMS	Root Mean Square
UDF	User-Defined Function
UDM	User-Defined Memory
VOF	Volume of Fluid

Symbols

c	Specific heat	[J/kgK]
c_p	Specific heat at constant pressure	[J/kgK]
g	Gravitational acceleration	[m/s^2]
h_{lv}	Latent heat	[J/kg]
H	Duct height	[m]
k	Sub-iteration	[–]
L	Plate length	[m]
$\dot{m}$	Mass flux	[kg/m^{2}s]
M	Current time-step	[–]
N	Scaling factor	[–]
p	Static pressure	[Pa]
Pr	Prandtl number	[–]
Re	Reynolds number	[–]
s	Plate thickness	[m]
S_ρ	Film continuity source term	[kg/m^{2}s]
$S_\mathbf{u}$	Film momentum source term	[kg/ms^2]
S_T	Film energy source term	[kgK/m^{2}s]
t	Time	[s]
$\bar{t}$	Pseudo time	[s]
T	Static temperature	[K]
u	x-velocity	[m/s]
v	y-velocity	[m/s]
v_{in}	Inlet velocity	[m/s]
w	z-velocity	[m/s]
W	Plate depth	[m]

Greek

δ	Film thickness	[m]
λ	Thermal conductivity	[W/mK]
μ	Dynamic viscosity	[Pa s]
ρ	Density	[kg/m^3]
τ	Characteristic time	[s]

Subscripts/Superscripts

amb	Ambient condition
$cond$	Condensation
$\delta/2$	Half-depth
f	Fluid
F	Film
l	Liquid
sat	Saturation
s	Solid
v	Vapor
w	Wall

CRediT authorship contribution statement

I. Rafanelli: Writing – review & editing, Writing – original draft, Software, Methodology, Investigation, Formal analysis, Conceptualization. **A. Andreini:** Validation, Supervision. **L. He:** Supervision, Methodology.

Declaration of competing interest

The authors declare that they have no known competing financial interests or personal relationships that could have appeared to influence the work reported in this paper.

Data availability

Data will be made available on request.

References

[1] I. Mudawar, Recent advances in high-flux, two-phase thermal management, J. Therm. Sci. Eng. Appl. 5 (2) (2013) 021012.
[2] I. Tanasawa, Advances in condensation heat transfer, in: Advances in Heat Transfer, vol. 21, Elsevier, 1991, pp. 55–139.
[3] M. Tancon, A. Abbatecola, S. Bortolin, L. Facco, R. Parin, D. Del Col, Dropwise-to-filmwise transition during condensation of steam on hydrophilic surfaces, Appl. Therm. Eng. (2025) 127128.
[4] K.-S. Cheong, A.D. Karstensen, Integrity assessment of an embrittled steam turbine casing, Int. J. Press. Vessels Pip. 86 (4) (2009) 265–272.
[5] G. Kosman, A. Rusin, The influence of the start-ups and cyclic loads of steam turbines conducted according to European standards on the component's life, Energy 26 (12) (2001) 1083–1099.
[6] J.H. Son, I.S. Park, Temperature changes around interface cells in a one-dimensional stefan condensation problem using four well-known phase-change models, Int. J. Therm. Sci. 161 (2021) 106718.
[7] T.-Y. Chen, R.D. Port, C.B. Batton, D. Cicero, Condensate corrosion in steam generating systems, in: NACE CORROSION, NACE, 1998, pp. NACE–98718.
[8] W. Nusselt, Die oberflachenkondensation des wasserdamphes, VDI-Zs 60 (1916) 541.
[9] J. Caldwell, Y. Kwan, Numerical methods for one-dimensional stefan problems, Commun. Numer. Methods Eng. 20 (7) (2004) 535–545.
[10] J.C. Chato, Laminar condensation inside horizontal and inclined tubes (Ph.D. thesis), Massachusetts Institute of Technology, 1960.
[11] A. Cavallini, R. Zecchin, A dimensionless correlation for heat transfer in forced convection condensation, in: International Heat Transfer Conference Digital Library, Begel House Inc., 1974.
[12] M.K. Dobson, J.C. Chato, Condensation in smooth horizontal tubes, 1998.
[13] J.R. Thome, J. El Hajal, A. Cavallini, Condensation in horizontal tubes, part 2: new heat transfer model based on flow regimes, Int. J. Heat Mass Transfer 46 (18) (2003) 3365–3387.
[14] M.M. Shah, An improved and extended general correlation for heat transfer during condensation in plain tubes, Hvac&R Res. 15 (5) (2009) 889–913.
[15] D. Sun, J. Xu, Q. Chen, Modeling of the evaporation and condensation phase-change problems with FLUENT, Numer. Heat Transfer B 66 (4) (2014) 326–342.
[16] W.H. Lee, A pressure iteration scheme for two-phase flow modeling, Multiph. Transp. Fundam. React. Saf. Appl. 1 (1980) 407–431.

[17] R. Szijártó, Condensation of steam in horizontal pipes: model development and validation, Tech. rep., Swiss Federal Institute of Technology ETH.
[18] S. Hardt, F. Wondra, Evaporation model for interfacial flows based on a continuum-field representation of the source terms, J. Comput. Phys. 227 (11) (2008) 5871–5895.
[19] T. Tandon, H. Varma, C. Gupta, A new flow regimes map for condensation inside horizontal tubes, 1982.
[20] L. He, Conjugate heat transfer: Some fundamentals and recent progress, Adv. Heat Transf. 55 (2023) 41–87.
[21] L. He, M. Fadl, Multi-scale time integration for transient conjugate heat transfer, Internat. J. Numer. Methods Fluids 83 (12) (2017) 887–904.
[22] I. Rafanelli, A. Andreini, B. Facchini, T. Diurno, S.G. Tomasello, G. Girezzi, Development and validation of a numerical multiphysics algorithm for wall condensation heat transfer for steam turbines starting phases, in: Turbo Expo: Power for Land, Sea, and Air, vol. 88018, American Society of Mechanical Engineers, 2024, V009T20A006.
[23] G. Gimenez, M. Errera, D. Baillis, Y. Smith, F. Pardo, A coupling numerical methodology for weakly transient conjugate heat transfer problems, Int. J. Heat Mass Transfer 97 (2016) 975–989.
[24] Y. Shi, S. Ding, T. Qiu, C. Liu, S. Zhang, Bi-fo time scaling method in the numerical simulation of transient conjugate heat transfer, Propuls. Power Res. 10 (3) (2021) 209–223.
[25] M. Fadl, L. He, P. Stein, G. Marinescu, Assessment of unsteadiness modeling for transient natural convection, J. Eng. Gas Turbines Power 140 (1) (2018) 012605.
[26] R. Ingle, R. Yadav, H. Punekar, J. Cao, Modeling of particle wall interaction and film transport using Eulerian wall film model, in: Gas Turbine India Conference, vol. 49644, American Society of Mechanical Engineers, 2014, V001T03A006.
[27] H. Narkhede, P. Dhamangaonkar, K. Parashar, CFD simulation for condensation of humid air over vertical plate with Eulerian wall film approach, in: Recent Advances in Fluid Dynamics: Select Proceedings of ICAFFTS 2021, Springer, 2022, pp. 425–439.
[28] Lee, The Effects of Noncondensable Gas on Steam Condensation in a Vertical Tube of Passive Residual Heat Removal System (Ph.D. thesis), 2008.
[29] N.H. Paul, N.R. Atkins, T. Brandvik, A scalable conjugate heat transfer method applied to engine transients, in: Turbo Expo: Power for Land, Sea, and Air, vol. 88070, American Society of Mechanical Engineers, 2024, V12CT32A052.